ACS OMEGA

http://pubs.acs.org/journal/acsodf

Article

Evaluating the Effect of Ionic Liquid on Biosorption Potential of Peanut Waste: Experimental and Theoretical Studies

Amna Bibi, Sadia Naz,* and Maliha Uroos*

Cite This: *ACS Omega* 2021, 6, 22259−22271

Read Online

ACCESS | Metrics & More | Article Recommendations

ABSTRACT: Peanut skin having polyphenols as major constituents is a natural, abundant, and environmentally friendly potent biosorbent for aquatic pollutants such as heavy metals. Its natural potential can be enhanced several times by treating it with ionic liquids—the green solvents. This report presents a complete study on biosorption of divalent cadmium ions using ionic liquid-treated peanut skin. Initially, both peanut biomasses, skin and shells, were tested, and peanut skin was used for thorough experimentation because of its higher adsorption potential (q_e values). Ionic liquids are highly green and designed solvents with vast adjustable striking features such as high thermal and chemical stability, insignificant vapor pressure, wide electrochemical assortment, non-volatility, non-flammability, less toxicity, and high recycling ability. Peanut skin after treatment with ionic liquids was characterized via FTIR, TGA, SEM, and XRD. The biosorption process was optimized with respect to time, temperature, metal ion concentrations, agitation speed, pH, and adsorbent dose. Data obtained were interpreted by kinetic, isothermal, and thermodynamic models. The biosorbent and ionic liquid both are regenerated and recycled up to three times, so cost effectiveness is a promising thing.

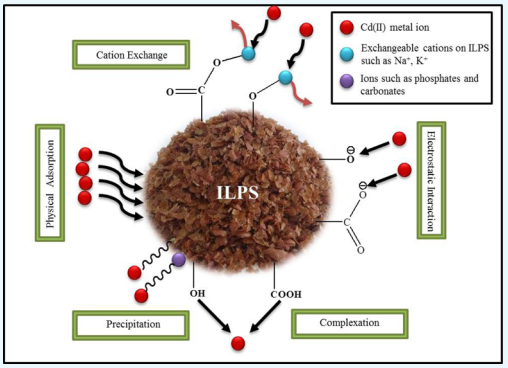

1. INTRODUCTION

Ionic liquids are a special class of molten organic salts, exhibiting melting points less than 100 °C. They are composed of organic cations and an organic or inorganic anion bound together via weak electrostatic interactions. They are highly designed solvents with infinite modifiable prominent features such as extensive electrochemical assortment, insignificant vapor pressure, and high thermal stability. Some other distinguished properties are polarity, viscosity, hygroscopicity, and high solvating power; even they can dissolve polymeric compounds. These properties can be adjusted accordingly by careful choice of the anion or cation.[1] In view of rapidly emerging green chemistry and clean technology, applications of ionic liquids (ILs) in various fields are constantly being explored by researchers.[2,3] One of such applications is water purification. ILs are reported to get rid of contaminants such as heavy metals, dyes, and other toxic compounds from water both by extraction and by adsorption mechanism.[4] Among all the pollutants, heavy metals are the most common, exhibiting bio-accumulative property. Mina Mata and itai-itai are two of many diseases caused by heavy metals, which made history. Mining activities, agricultural runoff, industrial discharge, and household applications are the main sources of heavy metal release into the nearby water bodies.[5] Cadmium is one of the hazardous heavy metals causing human health disorders if it exceeds the recommended uptake limit by the World Health Organization. It is mainly used in paints, photography, and rechargeable batteries along with another heavy metal, nickel. It is present primarily in urban wastewater where waste of detergents, body care products, and food products is present largely.[6] It can easily and readily enter into the food chain without exhibiting any positive impacts on the food chain. It affects the female reproductive system and damages the nervous system and kidneys.[7] Therefore, its efficient removal from waste water should be done with prime focus.

Up to now, various conventional treatment processes such as ion exchange,[8] chemical precipitation,[3] electrodialysis,[9] reverse osmosis,[10] coagulation and flocculation,[11,12] flotation,[13] and electrochemical treatment[14] methods have been reported to take away heavy metals from water. Requirement of large chemical quantities, residual solubility of metals, high capital investment, and running cost and generation of a large amount of sludge are the main disadvantages of these methods.[15] Adsorption is the only versatile, advanced, and most widely used technique for metal removal due to flexibility in its design and operation and cost effectiveness.[16] A number of common

Received: June 6, 2021
Accepted: August 9, 2021
Published: August 20, 2021

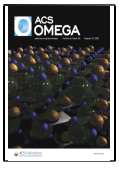

https://doi.org/10.1021/acsomega.1c02957
ACS Omega 2021, 6, 22259−22271

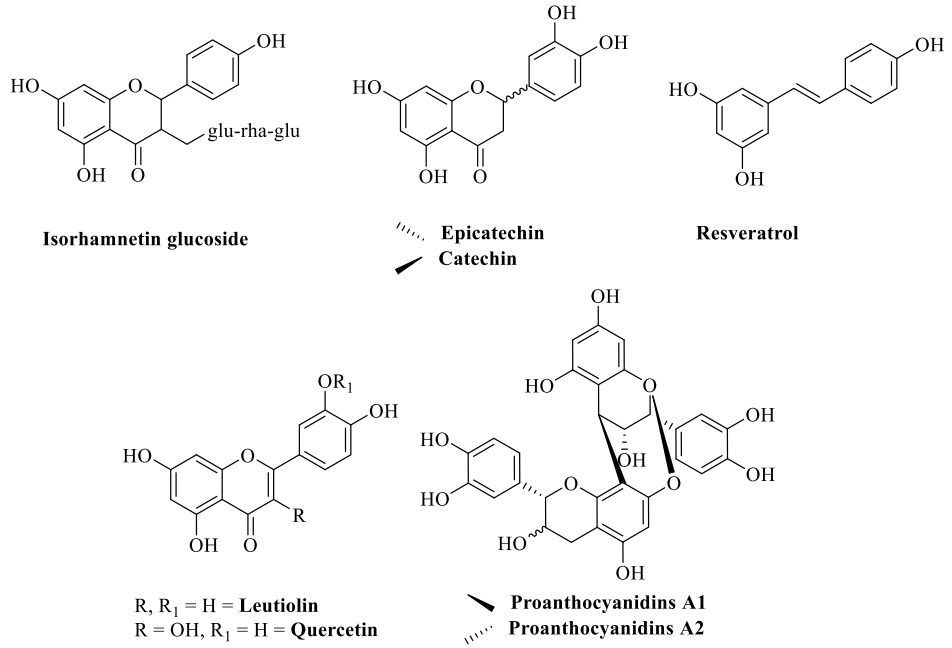

Figure 1. Some representative polyphenolic constituents of PS.

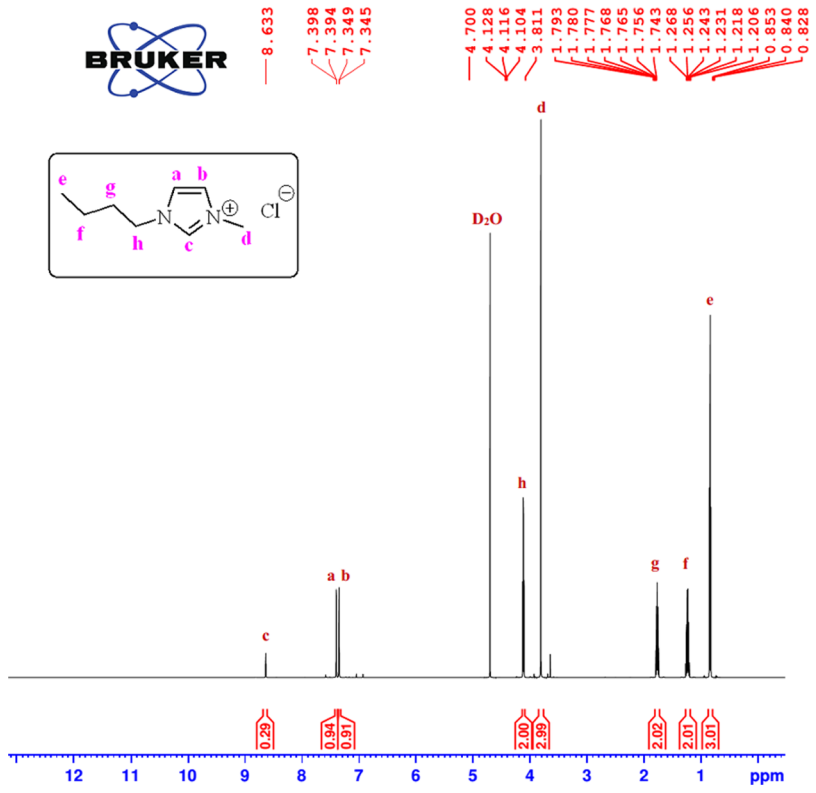

Figure 2. [1]HNMR of synthesized 1-butyl-3-methylimidazolium chloride ($[C_4C_1IM]Cl$) IL.

agricultural waste materials and natural polymers have been reported as effective biosorbents for removal of heavy metals in the recent literature.[17−21] Likewise, peanut husk (PH) can serve as a potent biosorbent for heavy metals.[22] PH comprises the lignocellulosic peanut shell and polyphenolic peanut skin (PS). The lignocellulosic peanut shell contains cellulose, hemicellulose, lignin, extractives, and ashes, while PS is composed of proteins, fats, carbohydrates, and polyphenols (Figure 1).[23] Phenolic acids, flavonoids, resveratrol,[24] catechins, A-type procyanidins, B-type procyanidin dimmers, procyanidin trimers, tetramers, and oligomers with higher polymerization degrees[25] are responsible for active functional sites for metal adsorption.

In contrast to various chemicals used for enhancing the adsorption potential of lignocellulosic adsorbents, we tried ILs in view of their extensive green profile and eco-friendly behavior. They exhibit strong ability to enhance the properties of various functional materials by modifying their surfaces

https://doi.org/10.1021/acsomega.1c02957
ACS Omega 2021, 6, 22259−22271

when combined with them. It extends their applicability in different fields of chemistry.[26]

We used ILs to enhance the biosorption potential of both the PS and shells for cadmium metal. 1-Butyl-3-methylimidazolium chloride [C_4C_1IM]Cl is selected as it is the most widely explored IL for a number of applications; it has a wide range of applications in synthesis and catalysis,[2] oxidation and depolymerization of natural biopolymers,[1] extraction of lignin from lignocellulose,[27] conversion of agricultural waste into platform chemicals and biofuel,[28] extractive desulfurization of liquid fuel,[29] and in many other fields. Therefore, we selected a commonly known and well-explored IL for this study before using any other novel one. Different parameters that may affect the adsorption percentage are also optimized. Kinetic, thermodynamic, and isothermal behaviors of the process are also studied.

2. RESULTS AND DISCUSSION

2.1. ^{1}HNMR Analysis of IL. ^{1}HNMR of synthesized [C_4C_1IM]Cl was recorded in D_2O at 600 MHz, Bruker's AVANCE Neo Technology (Figure 2). Imidazolium ring protons at C4 and C5 appeared as doublets at 7.39 and 7.35 ppm with coupling constants of 2.4 Hz, respectively. The C2 ring proton appeared as a singlet at 8.63 ppm. *N*-Methyl protons substituted at C3 of imidazolium appeared as a singlet at 3.81 ppm, while *N*-butyl protons substituted at C1 of imidazolium appeared as two triplets and two multiplets at 0.83, 1.20, 1.74, and 4.10 ppm.

2.2. IL Functionalization of Peanut Biomass. The peanut skin (PS), peanut shells and husk (both skin and shells) were functionalized by IL 1-butyl-3-methylimidazolium chloride ([C_4C_1IM]Cl). The IL was first dried completely, and then, finely powdered PS, shell, and husks were dissolved into it at 80, 100, 120, and 140 °C. From all these temperatures, 100 °C was selected as the optimum one, as higher temperatures caused carbonization of biomass. A maximum of 10 wt % biomass was loaded into the IL in view of maximum dissolution capacity of IL; increasing the amount of biomass caused too much saturation. One hour time was given for the reaction based on the maximum dissolution of biomass in IL. Also, increasing the time caused the blackening of the reaction mixture that is not advisable. After the maximum dissolution of biomasses into the IL, they are regenerated by addition of anti-solvents; an equimolar water and acetone mixture was used.[30] Regenerated functionalized biomass was washed quite a lot of times with deionized water and dried up well.

2.3. Characterization of the Adsorbent. *2.3.1. FTIR Analysis.* Fourier transform infrared (FTIR) analyses of the PS, IL-functionalized PS (ILPS), and cadmium-adsorbed ILPS were recorded to observe the biosorbent's structural functionalities (Figure 3). PS was observed to have characteristic peaks of hydroxyl, carbonyl, ether, and alkene functional groups. After IL treatment and cadmium adsorption, same peaks are observed with slight peak shifts. The peak shift is more apparent for band stretching of the −OH group (Table 1).

2.3.2. TGA Analysis. Three different thermal decomposition regions were observed from the thermogravimetric analysis (TGA) profile of ILPS (Figure 4); 22−58, 58−220, and 220−366 °C. The first region corresponds to the loss of any possible water physically present in the adsorbent, and it depicts just 10% weight loss. The other two regions depict two major

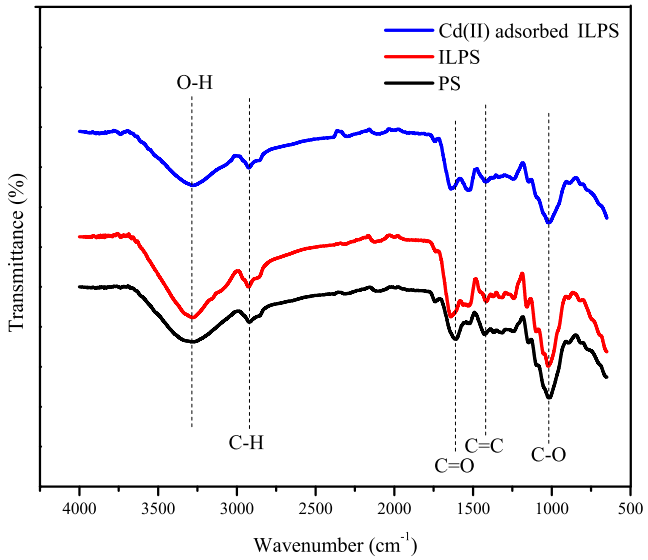

Figure 3. FTIR analysis of PS, ILPS, and cadmium-adsorbed ILPS.

Table 1. Assignment of Peaks in FTIR Spectra of Adsorbents before and after Adsorption

wavenumber (cm^{-1})			
PS	ILPS	ILPS after adsorption	assignment
3301	3295	3301	−OH stretching
2941	2943	2942	−CH stretching
1636	1653	1652	C═O stretching
1437	1436	1436	C═C stretching
1034	1036	1035	−C−O

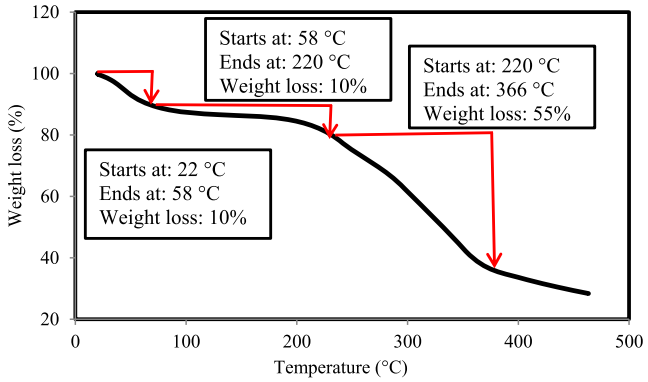

Figure 4. TGA of ILPS.

degradation phases that may be conforming to both the decomposition of the PS and degradation of the polymer matrix.[31] The second region exhibits 10 wt % loss at 58−220 °C temperature. The main loss of weight (55%) is observed in the last region (220−366 °C), in which the adsorbent is decomposed.

2.3.3. SEM Analysis. The morphology of the ILPS adsorbent was noted via scanning electron microscopy (SEM) images. Micrographs were taken at 50, 25, 10, and 5k× magnifications for 500 nm and 1, 2, and 5 μm particle sizes (Figure 5). All these images show a highly porous disrupted sheet of adsorbent with a rough flaky surface. This rough flaky surface facilitates the attachment of metal ions, thus enhancing the adsorption process. The porosity of the biosorbent also expedites its interaction with the adsorbate.[27,30]

https://doi.org/10.1021/acsomega.1c02957
ACS Omega 2021, 6, 22259−22271

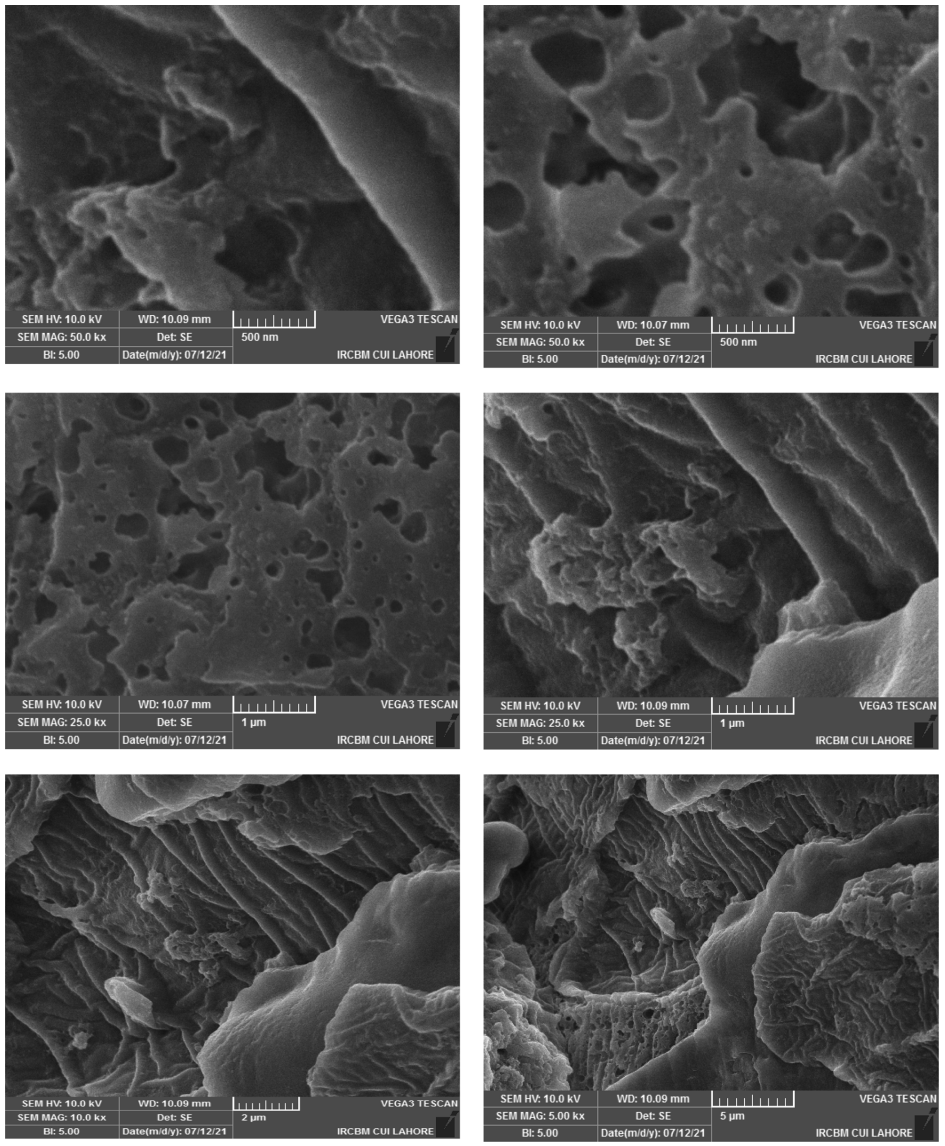

Figure 5. SEM images of ILPS at different sizes; 500 nm and 1, 2, and 5 μm.

2.3.4. XRD Analysis. To determine the crystallinity of ILPS, X-ray diffraction (XRD) analysis was carried out. A Bragg peak appeared at the 22° 2θ value corresponding to the (100) plane, revealing the simple cubic structure of the biosorbent (Figure 6).

2.4. Effect of Various Parameters on Adsorption Rate. *2.4.1. Screening of Peanut Biomass as a Biosorbent.* To check the efficiency of peanut biomasses for Cd(II) adsorption, PH and separate components, skin and shell, both untreated and treated with ILs, were screened in test experiments. All four experimental setups were given the same conditions; 20 mg of all biomasses was brought in contact with 30 mL of 20 ppm metal solutions at neutral pH and shaken at 150 rpm for 1 h at room temperature. It was observed that ILPS was the most efficient amongst all, as is observed by its adsorption efficiency (Figure 7). After ILPS, the second-highest adsorption potential was that of IL-modified shells. Then, the turns are of PS, PH, and the peanut shell. The reason for the highest adsorption potential of ILPS may be clarified on the basis of the polyphenolic structure of PS saturated with −OH functionalities. When treated with IL, Cl^- of $[C_4C_1IM]Cl$ dissolves these −OH functionalities by hydrogen bonding. When water is added as a co-solvent, it tends to break up this hydrogen bonding and make its own bonding with Cl^-, thus dissolving the IL in itself and causing PS to regenerate (Figure 8). This regenerated ILPS is now functionalized with IL with a refined morphology and reduced crystallinity, as is obvious by XRD and SEM, and of course, some unique properties are unidentified yet. FTIR spectra also confirm that there is no chemical change in the structure of peanut biomass after IL functionalization; there is just a change in peak areas of −OH, confirming the disruption of hydrogen bonding.

On the other hand, the shell comprises cellulose, hemicellulose, lignin, and some percentage of extractives and ashes. When treated with IL, this lignocellulose is dissolved in the IL, and then, water and acetone in equal proportions were added to regenerate cellulose and lignin. Water helps in regeneration of cellulose, while the lignin gets dissolved in acetone and goes with the filtrate fraction containing IL, water, and acetone. Thus, the enhanced adsorption capacity of this regenerated cellulose-rich material or IL-functionalized peanut shell can be attributed to the reduced crystallinity of the delignified shell.

https://doi.org/10.1021/acsomega.1c02957
ACS Omega 2021, 6, 22259−22271

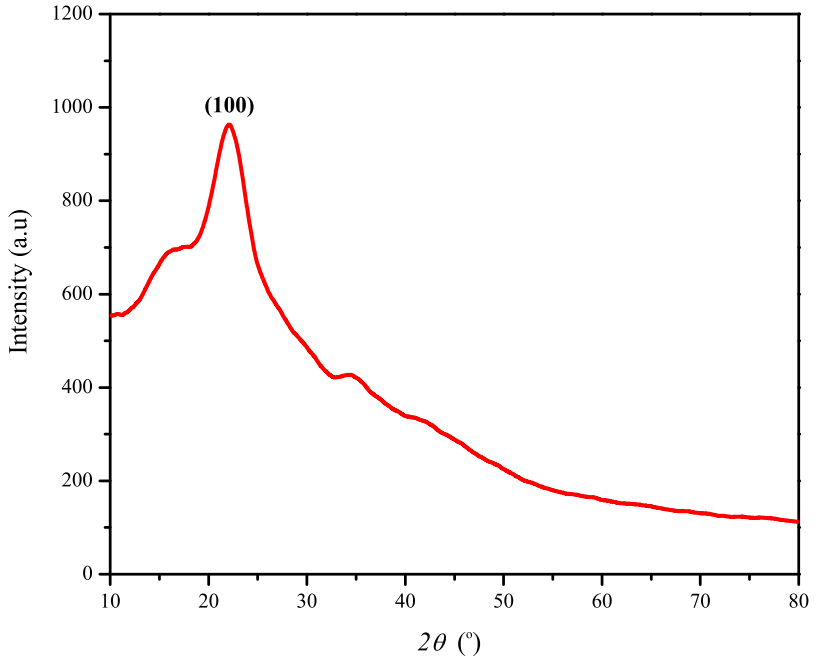

Figure 6. XRD analysis of ILPS.

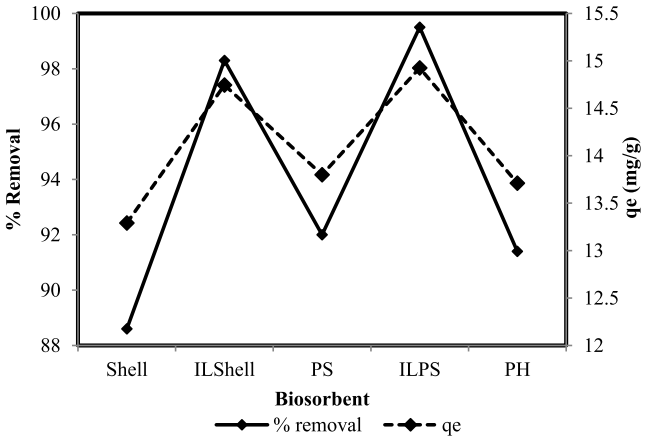

Figure 7. Screening of untreated and IL-functionalized peanut biomasses for Cd(II) biosorption. Shell (untreated peanut shell), IL Shell (IL-functionalized peanut shell), PS (peanut skin), ILPS (IL-functionalized PS), and PH (peanut husk).

Hence, IL is the efficient medium to enhance the adsorption capacities of polyphenolic compounds and lignocellulosics.

2.4.2. Effect of Initial Metal Ion Concentrations: Equilibrium Isotherms. The effect of initial metal ion concentration was studied using different concentrations of cadmium metal solutions with 30 mg of ILPS in each solution. These solutions were then shaken at 150 rpm for 1 h at room temperature. The results indicated that the percentage removal of metal declines with the rise in the initial concentration, while metal uptake capacity of the adsorbent increases with the increase in metal concentration (Figure 9). This can be attributed to the less availability of adsorption sites after optimum concentration.[32] The optimum concentration for metal removal was 20 ppm; all other parameters were studied at this concentration.

The amount of metal ions adsorbed by ILPS, equilibrium between ILPS and metal Cd(II) solution, and mechanistic parameters associated with the adsorption of metal ions were inspected by adsorption isotherms—Langmuir, Freundlich, and Temkin.

The Langmuir isotherm assumes that there are a fixed number of homogeneously distributed active sites that have the same affinity for adsorption of a monolayer having no mutual interactions. At the equilibrium point, due to saturation, there is no further adsorption.[33] It can be expressed as

$$\frac{C_e}{q_e} = \frac{C_e}{q_{max}} + \frac{1}{K_L q_{max}} \quad (1)$$

where q_e (mg g^{-1}) is the metal amount adsorbed at equilibrium, q_{max} (mg g^{-1}) is the capacity of monolayer sorption, C_e is the concentration of metal ions in solution at equilibrium, and K_L is the Langmuir constant. The essential characteristic of the Langmuir isotherm can be expressed by the dimensionless constant called the equilibrium parameter R_L defined by

$$R_L = \frac{1}{1 + K_L C_o} \quad (2)$$

where "K_L" is the constant of Langmuir and C_o (mg L^{-1}) is the initial metal ion concentration. It points to the feasibility and shape of the isotherm. The value of R_L indicates the type of isotherm to be unfavorable ($R_L > 1$), linear ($R_L = 1$), irreversible ($R_L = 0$), or favorable ($0 > R_L > 1$).

The value of the correlation coefficient R^2 which is regarded as a measure of the goodness of fit of experimental data on the isotherm is closer to 0.99, indicating a very good mathematical fit. The R_L value also lies between zero and one, showing that adsorption of Cd(II) by ILPS follows the Langmuir isotherm model.

The Freundlich isotherm considers the non-ideal adsorption in a multilayer fashion on heterogeneous surfaces of the adsorbent. Its linear mathematical expression is as follows[34]

$$\ln q_e = \frac{1}{n}(\ln C_e) + \ln K_f \quad (3)$$

https://doi.org/10.1021/acsomega.1c02957
ACS Omega 2021, 6, 22259−22271

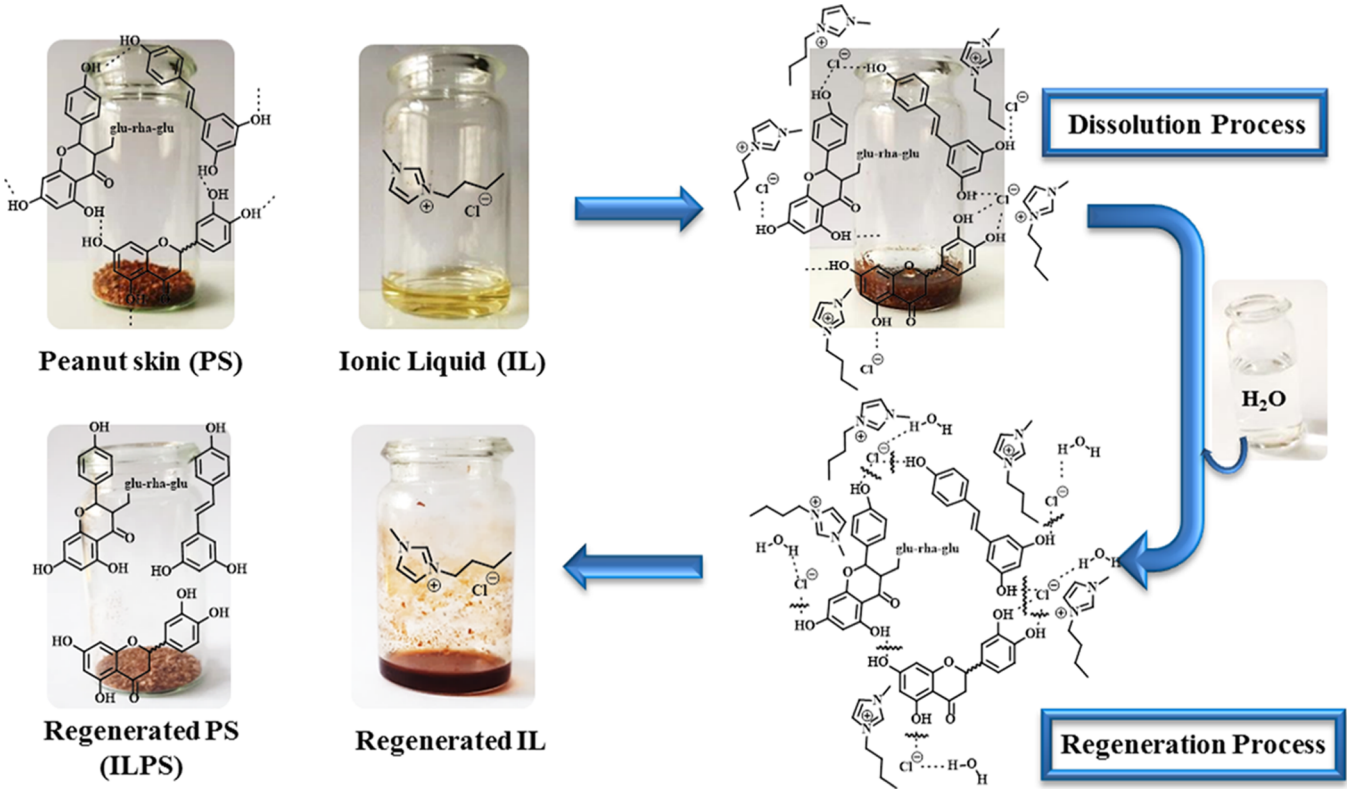

Figure 8. Mechanism for functionalization of PS with IL.

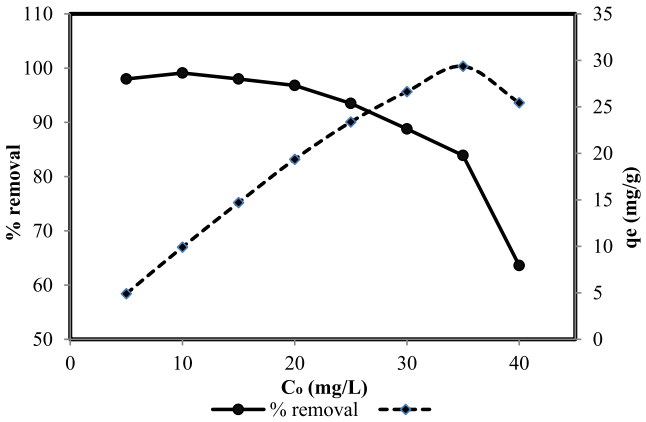

Figure 9. Effect of initial concentrations of Cd(II) on removal efficiency.

where $1/n$ and K_f are Freundlich constants.

At different concentrations, the plotted parameters show a linear relation to each other (Figure 10). Comparing the R^2 values for both the Langmuir and Freundlich isotherms, it was confirmed that the Langmuir isotherm fitted the best to describe the equilibrium data for metal removal by ILPS at the different initial concentrations.

According to the Temkin model, adsorption is regarded as an unvarying dispersal of binding energies up to the maximum binding energy[35] and follows the following equation

$$q_e = B \ln K_T + B\ln C_e \quad (4)$$

where B and K_T are constants. It may be concluded from the correlation coefficient (Table 2) that the equilibrium data are very well represented by the Temkin isotherm. It exhibits that Cd(II) adsorption is categorized by an even scattering of binding energies up to some maximum binding energy.

2.4.3. Effect of Adsorbent Dosage. Different amounts of biosorbents added to the batch biosorption process produce varying results of percentage removal and equilibrium adsorption capacity. Hence, it is important to screen a particular range of biosorbent dosages against other fixed factors to select the optimum amount of the biosorbent for all-out possible metal ion removal under an optimum set of conditions.

In view of high-adsorption results of the IL-functionalized peanut shell and skin, both these biomasses were tested for dose optimization and to countercheck the best biomass for later factors. Different dosages of the functionalized PS and shell (10, 20, 30, 40, and 50 mg) were added in 20 ppm metal solution (30 mL) and shaken at 150 rpm for 1 h at room temperature. The graph plotted between percentage removal, equilibrium adsorption capacity, and adsorbent dose (Figure 11) revealed that the percentage removal of metal ions proliferates with the adsorbent dose till optimum dosage, after which the percentage removal becomes almost constant. This decrease in the biosorbent's adsorption tendency after the optimal limit can be attributed to the self-aggregation of the biosorbent, due to which reduction of active sites may happen for adsorption.[36] Another reason is the inter-particle interactions due to the high amount of the adsorbent, causing a decrease in the adsorbent's total surface area and a rise in the diffusional path length.[37] The optimum dose concluded from the graph was 40 mg, and this dose was used to study the next parameters. Adsorption potentials of biosorbents and percentage removal of metals also justified the previous findings; ILPS has greater adsorption capacity for Cd(II) as compared to the functionalized shell.

https://doi.org/10.1021/acsomega.1c02957
ACS Omega 2021, 6, 22259−22271

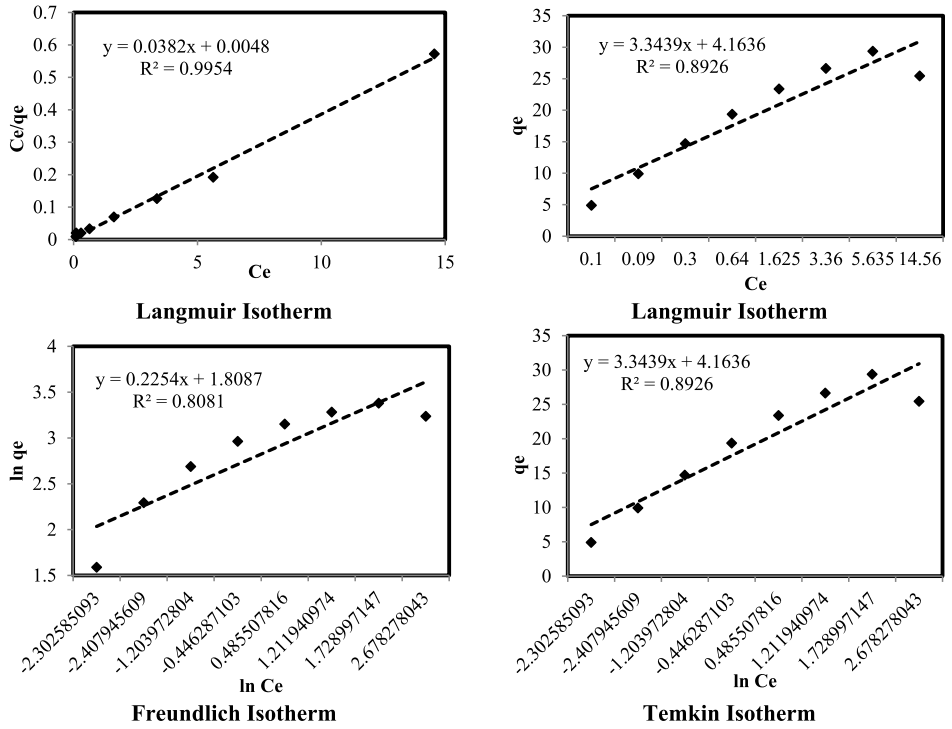

Figure 10. Sorption isothermal behavior of adsorption of Cd(II) over ILPS.

Table 2. Isotherm Constants of Langmuir, Freundlich, and Temkin Models

Langmuir isotherm				Freundlich isotherm			Temkin isotherm		
q_m (mg/g)	K_L (mg/L)	R^2	R_L	K_f	n	R^2	K_T	B_1	R^2
26.17	7.960	0.9954	0.006	6.1025	4.4365	0.8081	3.4732	3.3439	0.8926

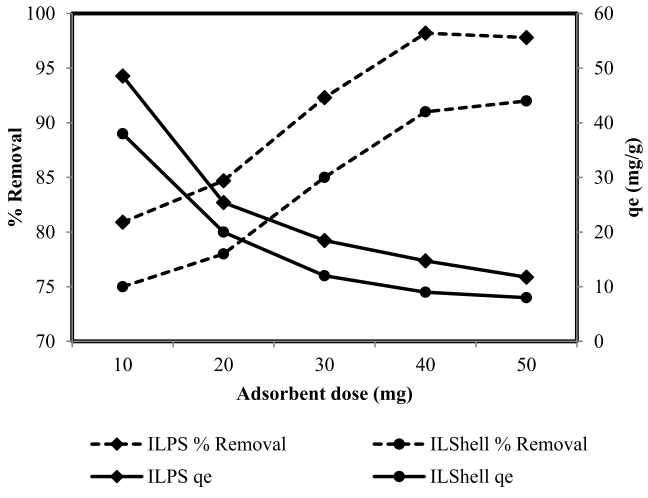

Figure 11. Effect of the IL-functionalized peanut shell and skin dosage on percentage removal of cadmium(II) and adsorption capacity.

2.4.4. Effect of Agitation Speed. The agitation dependence of the metal adsorption by ILPS was studied at different agitation speeds (30−180 rpm). An initial cadmium concentration of 20 ppm and 40 mg adsorbent dose were used for the experimentation, and 1 h shaking time was used for all the flasks at room temperature. It was observed that the adsorption potential of ILPS for Cd(II) was significantly increased as the agitation speed increased from 30 to 120 rpm; however, above this speed, adsorption potential decreased dramatically (Figure 12). Hence, the agitation speed influences the adsorption rate but up to a certain limit. The rationale for this result can be provided by considering the contact time and possibility of contact between the biosorbent and metal ions in solution, as stirring the solution at too much speed lowers the two. Further experimentation was done at 120 rpm.

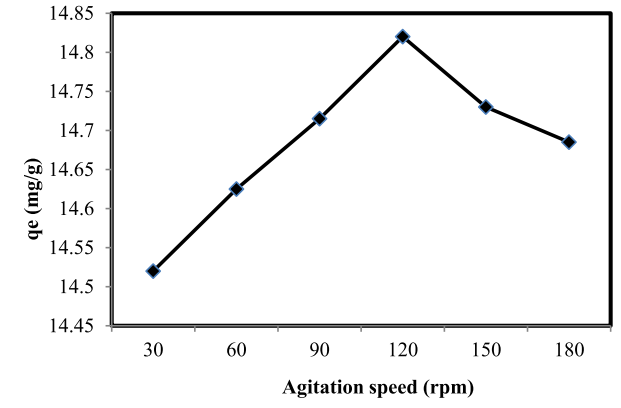

Figure 12. Effect of rpm on adsorption capacity of ILPS.

2.4.5. Effect of Solution pH. The pH of solution prepared for adsorption is one of the most significant parameters affecting the adsorption capacity of biosorbents. By changing the pH, the number of unsaturated sites available for adsorption is changed due to the variations in the ionic state of the adsorbent and its functional group activation.[38]

https://doi.org/10.1021/acsomega.1c02957
ACS Omega 2021, 6, 22259−22271

ILPS comprises different functional groups, as evidenced by FTIR. All these functionalities work differently at different pH values. In order to study the effect of pH on the adsorption efficiency of ILPS, batch experiments were conducted at different pH values. The Cd(II) uptake increased by increasing the pH from 2 to 8. At almost neutral pH (6−8), the adsorption capacity of ILPS for Cd(II) was maximum (Figure 13), suggesting that the adsorbent is efficient under near-

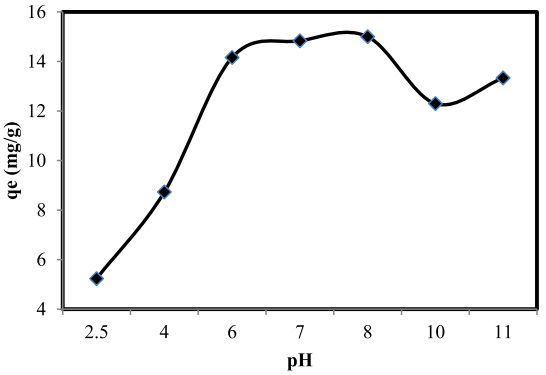

Figure 13. pH effect on the adsorption capacity of ILPS.

neutral pH conditions. pH can affect the protonation of functional groups in the biosorbent, along with the chemistry of the metal (i.e., its solubility). The higher adsorption at pH 6 might be due to the formation of negative active sites on the surface of the biosorbent that enhances the sorption by an electrostatic interaction between positively charged metal and the negatively charged biosorbent surface. Increasing the pH more than 8 decreases the biosorbent capacity that might be attributed to the precipitation of cadmium ions due to the formation of hydroxide. Different biosorbents are reported to behave the same.[39,40] At lower pH, due to high-acidic conditions, concentration of positive ions is enhanced that repel the positively charged metal ions in the solution, thus lowering the adsorption capacity.

2.4.6. Effect of Temperature: Thermodynamic Study. Biosorption is highly affected by temperature variations due to the endothermic and exothermic nature of adsorption onto the biosorbent. Therefore, the experimentation was done to find the optimum temperature to achieve the maximum Cd(II) adsorption by ILPS at optimum biosorbent dose, agitation speed, and initial metal ion concentration. Experiments were conducted at room temperature (RT), 308, 313, 333, 353, and 373 K with 40 mg of adsorbent and 20 ppm metal ion solution shaken at 120 rpm for 1 h. Maximum adsorption was observed at RT, above which the adsorption efficiency of ILPS starts to decrease (Figure 14). This can be due to the destruction of some polymeric active sites or the deactivation of the ILPS surface due to bond rupture.

Thermodynamic parameters, ΔG° (Gibbs free energy), ΔH° (standard enthalpy), and ΔS° (standard entropy), were calculated by the following equations

$$\Delta G^\circ = -\mathrm{RT} \ln K_\mathrm{D} \quad (5)$$

$$K_\mathrm{D} = \frac{C_\mathrm{o} - C_\mathrm{e}}{C_\mathrm{e}} \quad (6)$$

$$\Delta G^\circ = \Delta H^\circ - T\Delta S^\circ \quad (7)$$

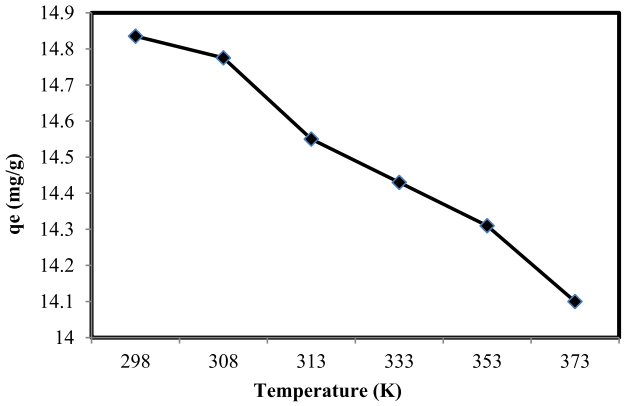

Figure 14. Influence of temperature on ILPS adsorption capacity.

where R is the universal gas constant, T is the temperature, and K_D is the constant of equilibrium calculated by eq 6. The positive values of ΔG° demonstrate the non-spontaneous behavior of the process (Table 3). Also, the values of ΔG°

Table 3. Thermodynamic Parameters for the Biosorption of Cd(II) on ILPS

temperature (K)	ΔG° (kJ mol^{-1})	ΔH° (kJ mol^{-1})	ΔS° (kJ mol^{-1})
298 (RT)	11.15	+7.89	+0.15
308	10.71		
313	9.04		
333	8.94		
353	8.90		
373	8.53		

were observed to decrease with increasing temperature, indicating the favorable binding at high temperatures. Standard entropy (ΔS°) and standard enthalpy (ΔH°) values were obtained by the intercept and slope using eq 7. Positive enthalpy values confirm the endothermic behavior of the process, while the positive values of ΔS° revealed a rise in disorderness at the interface of the solid and liquid.[41]

2.4.7. Effect of Time: Kinetic Study. Kinetic study helps in the determination of the adsorption mechanism. The effect of contact time between ILPS and cadmium metal ion solution was monitored, and adsorption capacity of ILPS for Cd(II) at different times is given in Figure 15. It can be seen that initially, there was a fast uptake of metal ions from 0 to 10 min and then, the highest uptake was observed at 30 min.

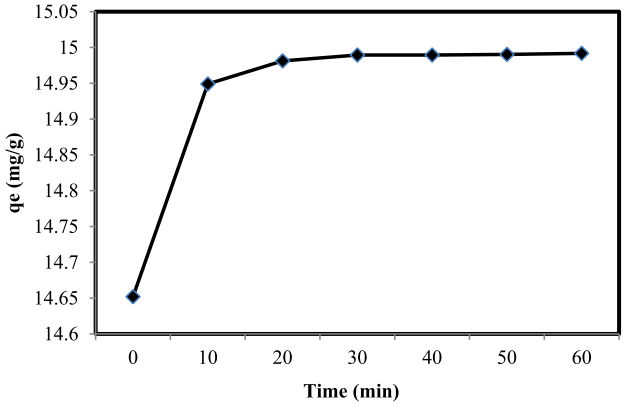

Figure 15. Effect of time on the adsorption capacity of ILPS.

https://doi.org/10.1021/acsomega.1c02957
ACS Omega 2021, 6, 22259−22271

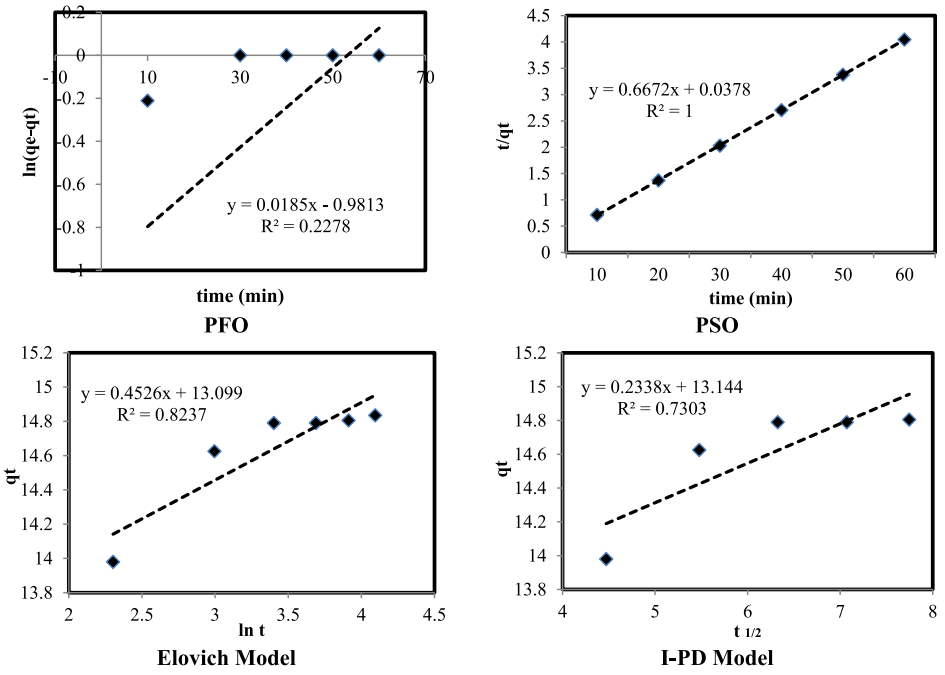

Figure 16. Kinetic models for biosorption of Cd(II) using ILPS.

Table 4. PFO and PSO Kinetic Rate Constants

PFO rate constants			experimental value	PSO rate constants		
K_1 (L min^{-1})	$q_{e(cal)}$ (mg g^{-1})	R^2	$q_{e(exp)}$ (mg g^{-1})	K_2 (mg g^{-1} min^{-1})	$q_{e(cal)}$ (mg g^{-1})	R^2
−0.0185	0.3748	0.2278	14.79	11.776	1.4988	1

Table 5. Rate Constants of Elovich and Intra-particle Diffusion Models

Elovich constants			intra-particle diffusion rate constant		
α (mg g^{-1} min^{-1})	β (g mg^{-1})	R^2	K_d (mg g^{-1} min^{-1})	C	R^2
13.099	0.4526	0.8237	0.2338	13.144	0.7303

Therefore, the adsorption capacity (q_e) of ILPS reached maximum at 30 min. At this point, the rate of adsorption is in dynamic equilibrium with the rate of desorption. After this optimal equilibrium time, no adsorption progress was observed.

The data obtained by this experimentation were used to plot kinetic models: PFO (pseudo-first-order) and PSO (pseudo-second-order) reaction models. According to the PFO model proposed in 1898 by Lagergren and Svenska, the rate of adsorption is proportional to the number of vacant sites left by the solutes.[42]

$$\ln(q_e - q_t) = \ln q_e - K_1 t \quad (8)$$

where q_t is the mg g^{-1} adsorption capacity of ILPS at any time t, q_e is the mg g^{-1} adsorption capacity of ILPS at equilibrium, and K_1 is the rate constant of the equation (min^{-1}).

The linear plot of $\ln(q_e - q_t)$ versus time in Figure 16 suggests that the Cd(II) adsorption process by ILPS did not follow the first-order kinetics. The values of K_1 and q_e calculated from the eq 7 and those of the correlation coefficient (R^2) fitting the PFO kinetic equation are shown in Table 4. It is clear from the table that the value of R^2 is just 0.2, suggesting that the process does not follow the PFO kinetic model.

The experimental data were then fitted to Ho and McKay's PSO kinetic equation,[43] which is

$$\frac{t}{q_t} = \frac{1}{K_2 q_e^2} + \frac{t}{q_e} \quad (9)$$

K_2 is the rate constant (g mg^{-1} min^{-1}) of the second-order equation. As obvious by the R^2 value of PSO calculated from the kinetic equation of t/q_t versus time plot, the adsorption process is well described by the PSO model (Figure 16; Table 4). Comparing the $q_{e(cal)}$ values of both models with $q_{e(exp)}$, the $q_{e(cal)}$ value of PSO is much more closer to it (Table 4), suggesting the second-order kinetics for the studied process. Thus, the sorption of cadmium metal onto ILPS is probable to be controlled by the chemisorption process.[44,45]

Elovich and intra-particle diffusion (I-PD) models were also applied to check the kinetics of the chemisorption process[46] and direct proportionality of metal uptake to $t_{1/2}$, as proposed by Weber and Morris[47]

$$q_t = \alpha + \beta \ln t \qquad \text{Elovich model}$$

$$q_t = K_d t^{1/2} + C \qquad \text{I-PD model}$$

where α represents the mg g^{-1} min initial sorption rate and β is related to the extent of surface coverage in g mg^{-1} and activation energy for chemisorption. The value of R^2 in the

https://doi.org/10.1021/acsomega.1c02957
ACS Omega 2021, 6, 22259−22271

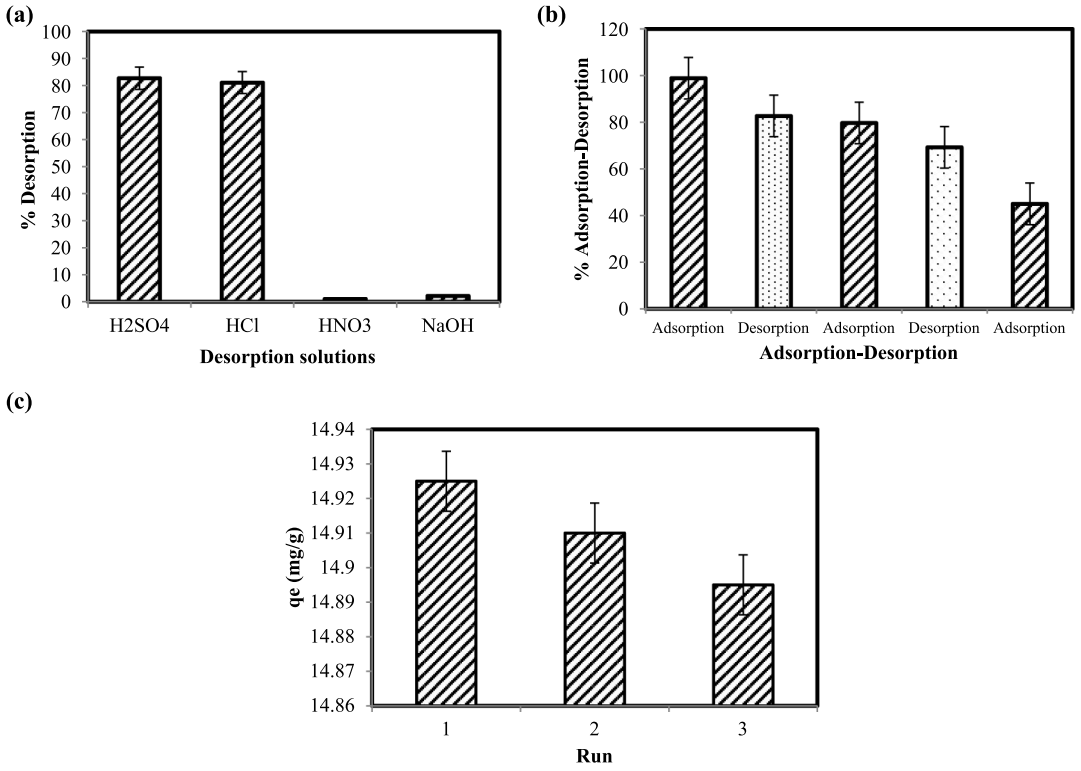

Figure 17. (a) Desorption and (b) reusing the desorbed biosorbent (c) and IL recycling.

Elovich model (Table 5) shows that adsorption is not chemisorption.

K_d in the I-PD model is the rate constant of intra-particle diffusion. C is the boundary layer thickness. If intra-particle diffusion takes place, the q_t versus $t_{1/2}$ will be linear. The rate-limiting process will be only due to intra-particle diffusion, if the plot is passing through the origin. Otherwise, some other mechanisms are also involved along with intra-particle diffusion. As the plot does not go through the origin (Figure 16d), the adsorption of Cd(II) on ILPS is not intra-particular diffusion-controlled.

3. DESORPTION AND RECYCLING STUDIES

Desorption is a practice of removing adsorbed metal from the surface of the adsorbent in order to regenerate it for second-batch experiments. This restoration and reuse of the adsorbent are imperative for making the biosorption cost-effective, dropping the reliance of the method on the continuous adsorbent supply, and also help in recovering the metal ions extracted from the liquid phase.[48] The common method for desorption of the heavy metals from the adsorbent is leaching with dilute acid. This is due to the fact that most biosorption processes follow an ion-exchange mechanism for metal ions, and thus, increasing the acidity of the metal-loaded adsorbent leads to the leaching of metal ions from the adsorbent.

To desorb our Cd(II)-loaded ILPS, 0.1 M solutions of H_2SO_4, HNO_3, HCl, and NaOH were tested under the same experimental conditions as those of adsorption. The desorbed amount of heavy metals (q_{de}) and desorption rate were calculated as follows by the following equations

$$q_{de} = \frac{C_1 \times V}{W} \tag{10}$$

$$\text{rate of desorption } \% = \frac{q_{de}}{q_e} \times 100 \tag{11}$$

where V is the volume of desorption solution (L), q_{de} (mg g^{-1}) is the desorbed amount of heavy metals, C_1 (mg L^{-1}) is the metal ion concentration of the desorption supernatant, and W_1 is the mass of the adsorbent. The results revealed that sulfuric acid and hydrochloric acids have greater desorption efficiencies as compared to nitric acid and sodium hydroxide (Figure 17a).

Further adsorption−desorption experiments were performed with H_2SO_4 based on its efficient desorption potential. Desorbed ILPS was used for the second-batch adsorption process and showed significant adsorption efficiency even for the third-batch adsorption (Figure 17b).

On the other hand, the eco- and cost effectiveness of this process lies in the reusability of regenerated IL. Regenerated IL can be used for treatment of fresh PS three times without significant efficiency loss (Figure 17c).

4. CONCLUSIONS

The positive effect of ionic liquid on adsorption efficiency of peanut biomass is described in this report. The PS and shells were treated with IL and then applied to adsorb cadmium(II) from aqueous media. Among all the adsorbents, the PS came up with the best adsorption potential after treatment with IL. All physical factors affecting the process were optimized. A total of 40 mg of adsorbent was enough for the adsorption of Cd(II) from its 20 ppm solution just in 30 min at 120 rpm. The adsorbent is efficient at 308 K temperature and near-neutral pH. Experimental data were also interpreted by kinetic, isothermal, and thermodynamic models. According to kinetic studies, the adsorption over the ILPS is a chemisorption process. Isothermal studies suggest that there are a fixed number of homogeneously distributed active sites onto the

https://doi.org/10.1021/acsomega.1c02957
ACS Omega 2021, 6, 22259−22271

ILPS that have the same affinity for adsorption of a monolayer having no mutual interactions. Thermodynamic studies suggest the non-spontaneity of the process. The ionic liquid and ionic liquid-treated adsorbent both have high recycling ability, as obvious by desorption and recycling experiments.

5. MATERIALS AND METHODS

1-Methylimidazole (Sigma-Aldrich), 1-chlorobutane (Fisher Scientific), and cadmium chloride (Riedel-de Haën) were of analytical grade and used as such. Solvents such as *n*-hexane and ethyl acetate were purchased and used after distillation. PH was collected from the local market, peeled off to collect the PS, and thoroughly washed with tap water to remove any adhesive insoluble materials, dirt, and dust. It was then washed with deionized water to make it free from any ions due to regular water that may cause result variations, if present. It was then air-dried for about 48 h followed by 12 h of oven drying at 45 °C to remove any moisture residing in the PS. Once dried, the PS was crushed and ground.

5.1. Synthesis of 1-Butyl-3-methylimidazolium Chloride [C_4C_1IM]Cl. 1-Butyl-3-methylimidazolium chloride [C_4C_1IM]Cl was synthesized according to the literature with a slight modification.[49] In a 100 mL round-bottom flask, 1 equiv of 1-methylimidazole and 1-chlorobutane (1.1 equiv) were added, and the flask was fitted to a reflux condenser. The temperature of the reaction was set to 110 °C. The progress of synthesis of the IL was supervised via thin-layer chromatography using ethyl acetate: *n*-hexane system. After completion of reaction, washing of the product was done with ethyl acetate to remove any unreacted base.

FTIR (cm^{-1}): 3398 (stretching vibration peaks of *n*-butyl hydrogen), 1570, 1465 (imidazole ring skeleton vibration), 1166 (methyl hydrogen's deformation), 1166 (inner bending vibration of CH). ^{1}HNMR (600 MHz, D_2O): δ (ppm): 8.63 (1H, s, CH), 7.39 (1H, d, J = 2.4 Hz, CH), 7.35 (1H, d, J = 2.4 Hz, CH), 4.10 (2H, t, J = 7.2 Hz, CH_2), 3.81 (3H, s, CH_3), 1.74 (2H, m, CH_2), 1.20 (2H, m, CH_2), 0.83 (3H, t, J = 7.2 Hz, CH_3).

5.2. Chemical Treatment of Peanut Biomass. The fine powdered PS, peanut shell, and PH were functionalized by treating with IL 1-butyl-3-methylimidazolium chloride [C_4C_1IM]Cl. The oven-dried IL was taken in a vial, and 10 wt % peanut biomass was loaded into it. It was heated at 100 °C with continuous stirring at 90 rpm for an hour. After that, 20−30 mL of distilled water was added to regenerate biomass from the IL followed by filtration and excessive washing with deionized water. The IL was regenerated by water evaporation, while the modified adsorbent was dried and stored in an oven-dried vial.

5.3. Characterization of the Chemically Modified Adsorbent. The PS modified with the IL (ILPS) was characterized by FTIR, TGA, SEM, and XRD. FTIR analysis was done via the Agilent Cary 630 FTIR instrument having a 4000−400 cm^{-1} scanning range. TGA was done with Leco's TGA 701 from ambient to 800 °C with a heating rate of 10 °C/min in 3.5 L/m (low) flowing nitrogen gas. SEM was done via the Vega Tescon with variable pressure. Samples were made conductive by gold sputtering, and images were taken at different magnifications. XRD analysis was done using the Rigaku Tabletop XRD instrument using Cu Kα radiation (λ = 1.54 Å) with a scanning rate of 0.01°/s and scan speed of 1°/min in a 2θ range of 10−80°.

5.4. Batch Adsorption Studies. Stock solution (1000 ppm) of $CdCl_2{\cdot}H_2O$ was prepared in deionized water. Different initial concentration solutions of metal ions were prepared by dilution of stock solution. The pH values of solutions were attuned using 0.1 M NaOH and HCl.

Equilibrium isothermal studies were carried out in the batch method. Metal ion solutions (10−40 mg L^{-1}; 30 mL volume) were shaken for different times (0−60 min) with a constant amount of adsorbents (10−50 mg). After suitable time, solutions were filtered, and concentrations of the un-adsorbed metal ions in aqueous solutions were determined using a flame atomic absorption spectrometer (AAS) (PerkinElmer instruments, Analyst 100). The extent of adsorbed metal and percentage removal of metals by the modified PS was calculated by the following equations

$$\text{percentage removal} = \frac{C_o - C_e}{C_o} \times 100 \quad (12)$$

$$\text{adsorption capacity } q_e = \frac{(C_o - C_e)V}{m} \quad (13)$$

where C_o and C_e are initial and final concentrations (at equilibrium) of the metal ions in solution (mg g^{-1}), V is the volume of solution, and m is the adsorbent mass (mg).

All the batch extraction experiments were performed in triplicates, and results are reported as their mean values calculated using Microsoft Excel 2010. Graphs are plotted using the same software tools. Regression values (R^2) were analyzed to validate all the studied models.

5.5. Desorption Experiment. Adsorption experiments can be made economical when joined with desorption ones to recover the metal and reuse the adsorbent for further loading and unloading cycles. In order to study the desorption, a 30 mL solution of 20 ppm metal ions was equilibrated with 40 mg of ILPS and shaken in a rotary shaker for 30 min at a speed of 120 rpm. The solutions were filtered after adsorption, and metal concentration in the filtrate was analyzed. Then, the loaded ILPS was shaken with 30 mL of 0.1 M solutions of H_2SO_4, HNO_3, HCl, and NaOH for 30 min at a speed of 120 rpm in order to provide the same conditions to adsorption and desorption cycles. Solutions were filtered after desorption, metal concentration in the filtrate was analyzed, and the remaining adsorbent was reused for the second-batch adsorption. This adsorption−desorption course was repeated three times.

AUTHOR INFORMATION

Corresponding Authors

Maliha Uroos − *Centre for Research in Ionic Liquids, School of Chemistry, University of the Punjab, 54590 Lahore, Pakistan*; orcid.org/0000-0001-8757-4151; Email: malihauroos.chem@pu.edu.pk

Sadia Naz − *Centre for Research in Ionic Liquids, School of Chemistry, University of the Punjab, 54590 Lahore, Pakistan*; orcid.org/0000-0001-5290-3621; Email: sadia.phd.chem@pu.edu.pk

Author

Amna Bibi − *Centre for Research in Ionic Liquids, School of Chemistry, University of the Punjab, 54590 Lahore, Pakistan*

Complete contact information is available at: https://pubs.acs.org/10.1021/acsomega.1c02957

https://doi.org/10.1021/acsomega.1c02957
ACS Omega 2021, 6, 22259−22271

Notes

The authors declare no competing financial interest.

■ ACKNOWLEDGMENTS

This work was financially supported by Higher Education Commission (HEC), Pakistan, under the NRPU Research Grant, project no. 8639/Punjab/NRPU/R&D/HEC/2017 and TDF Research Grant, project no. TDF03-294. School of Chemistry, University of Punjab, is acknowledged for its support toward this project.

■ REFERENCES

(1) Naz, S.; Uroos, M. Ionic Liquids Based Processing of Renewable and Sustainable Biopolymers. *Biofibers and Biopolymers for Biocomposites*; Springer, 2020; pp 181−207.
(2) Vekariya, R. L. A review of ionic liquids: Applications towards catalytic organic transformations. *J. Mol. Liq.* **2017**, *227*, 44−60.
(3) Watanabe, M.; Thomas, M. L.; Zhang, S.; Ueno, K.; Yasuda, T.; Dokko, K. Application of ionic liquids to energy storage and conversion materials and devices. *Chem. Rev.* **2017**, *117*, 7190−7239.
(4) Ayati, A.; Ranjbari, S.; Tanhaei, B.; Sillanpää, M. Ionic liquid-modified composites for the adsorptive removal of emerging water contaminants: A review. *J. Mol. Liq.* **2019**, *275*, 71−83.
(5) Gautam, R. K.; Sharma, S. K.; Mahiya, S.; Chattopadhyaya, M. C. Contamination of heavy metals in aquatic media: transport, toxicity and technologies for remediation. *Heavy Metals in Water: Presence, Removal and Safety*; RSC, 2014; pp 1−24.
(6) Cabrini, T. M. B.; Barboza, C. A. M.; Skinner, V. B.; Hauser-Davis, R. A.; Rocha, R. C.; Saint'Pierre, T. D.; Valentin, J. L.; Cardoso, R. S. Heavy metal contamination in sandy beach macrofauna communities from the Rio de Janeiro coast, Southeastern Brazil. *Environ. Pollut.* **2017**, *221*, 116−129.
(7) Sipra, N. H.; Mahmood, Q.; Waseem, A.; Irshad, M.; Pervez, A. Assessment of heavy metald in wheat plants irrigated with contaminated wastewater. *Pol. J. Environ. Stud.* **2013**, *22*, 115−123.
(8) Alyüz, B.; Veli, S. Kinetics and equilibrium studies for the removal of nickel and zinc from aqueous solutions by ion exchange resins. *J. Hazard. Mater.* **2009**, *167*, 482−488.
(9) Cifuentes, L.; García, I.; Arriagada, P.; Casas, J. M. The use of electrodialysis for metal separation and water recovery from $CuSO_4$, H_2SO_4, Fe solutions. *Sep. Purif. Technol.* **2009**, *68*, 105−108.
(10) Mohsen-Nia, M.; Montazeri, P.; Modarress, H. Removal of Cu^{+2} and Ni^{+2} from wastewater with a chelating agent and reverse osmosis processes. *Desalination* **2007**, *217*, 276−281.
(11) El Samrani, A. G.; Lartiges, B. S.; Villiéras, F. Chemical coagulation of combined sewer overflow: heavy metal removal and treatment optimization. *Water Res.* **2008**, *42*, 951−960.
(12) Yuan, X. Z.; Meng, Y. T.; Zeng, G. M.; Fang, Y. Y.; Shi, J. G. Evaluation of tea-derived biosurfactant on removing heavy metal ions from dilute wastewater by ion flotation. *Colloids Surf.* **2008**, *317*, 256−261.
(13) Medina, B. Y.; Torem, M. L.; de Mesquita, L. M. S. On the kinetics of precipitate flotation of Cr III using sodium dodecylsulfate and ethanol. *Miner. Eng.* **2005**, *18*, 225−231.
(14) Heidmann, I.; Calmano, W. Removal of Zn (II), Cu (II), Ni (II), Ag (I) and Cr (VI) present in aqueous solutions by aluminium electrocoagulation. *J. Hazard. Mater.* **2008**, *152*, 934−941.
(15) Chen, H.; Wang, A. Kinetic and isothermal studies of lead ion adsorption onto palygorskite clay. *J. Colloid Interface Sci.* **2007**, *307*, 309−316.
(16) Sari, A.; Tuzen, M.; Soylak, M. Adsorption of Pb (II) and Cr (III) from aqueous solution on Celtek clay. *J. Hazard. Mater.* **2007**, *144*, 41−46.
(17) Lindholm-Lehto, P. Biosorption of heavy metals by lignocellulosic biomass and chemical analysis. *BioResources* **2019**, *14*, 4952−4995.
(18) Sarada, B.; Krishna Prasad, M.; Kishore Kumar, K.; Murthy, C. V. R. Biosorption of Cd^{+2} by green plant biomass, Araucaria heterophylla: characterization, kinetic, isotherm and thermodynamic studies. *Appl. Water Sci.* **2017**, *7*, 3483−3496.
(19) Aman, A.; Ahmed, D.; Asad, N.; Masih, R.; Abd ur Rahman, H. M. Rose biomass as a potential biosorbent to remove chromium, mercury and zinc from contaminated waters. *Int. J. Environ. Stud.* **2018**, *75*, 774−787.
(20) Thakur, V.; Sharma, E.; Guleria, A.; Sangar, S.; Singh, K. Modification and management of lignocellulosic waste as an eco-friendly biosorbent for the application of heavy metal ionssorption. *Mater. Today: Proc.* **2020**, *32*, 608−619.
(21) Asemave, K.; Thaddeus, L.; Tarhemba, P. T. Lignocellulosic-based sorbents: A Review. *Sustainable Chem.* **2021**, *2*, 271−285.
(22) Tahiruddin, N. S. M.; Ab Rahman, S. Z. Adsorption of lead in aqueous solution by a mixture of activated charcoal and peanut shell. *World J. Sci. Technol. Res.* **2013**, *1*, 102−109.
(23) Massie, B. J.; Sanders, T. H.; Dean, L. L. Removal of heavy metal contamination from peanut skin extracts by waste biomass adsorption. *J. Food Process Eng.* **2015**, *38*, 555−561.
(24) Yu, J. M.; Ahmedna, M.; Goktepe, I. Effects of processing methods and extraction solvents on concentration and antioxidant activity of peanut skin phenolics. *Food Chem.* **2005**, *90*, 199−206.
(25) Lazarus, S. A.; Adamson, G. E.; Hammerstone, J. F.; Schmitz, H. H. High-performance liquid chromatography/mass spectrometry analysis of proanthocyanidins in foods and beverages. *J. Agric. Food Chem.* **1999**, *47*, 3693−3701.
(26) Fan, T.; Zhao, C.; Xiao, Z.; Guo, F.; Cai, K.; Lin, H.; Liu, Y.; Meng, H.; Min, Y.; Epstein, A. J. Fabricating of high-performance functional graphene fibers for micro-capacitive energy storage. *Sci. Rep.* **2016**, *6*, 29534.
(27) Asim, A. M.; Uroos, M.; Naz, S.; Muhammad, N. Pyridinium protic ionic liquids: Effective solvents for delignification of wheat straw. *J. Mol. Liq.* **2021**, *325*, 115013.
(28) Eminov, S.; Wilton-Ely, J. D. E. T.; Hallett, J. P. Highly selective and near-quantitative conversion of fructose to 5-hydroxymethylfurfural using mildly acidic ionic liquids. *ACS Sustainable Chem. Eng.* **2014**, *2*, 978−981.
(29) Dharaskar, S. A.; Varma, M. N.; Shende, D. Z.; Yoo, C. K.; Wasewar, K. L. Synthesis , characterizatopm and application of 1-butyl-3-methylimidazolium chloride as green material for extractive desulfurization of liquid fuel. *Sci. World J.* **2013**, *2013*, 395274.
(30) Naz, S.; Uroos, M.; Asim, A. M.; Muhammad, N.; Shah, F. U. One-pot deconstruction and conversion of lignocellulose into reducing sugars by pyridinium-based ionic liquid−metal salt system. *Front. Chem.* **2020**, *8*, 236.
(31) Khan, A. S.; Man, Z.; Bustam, M. A.; Nasrullah, A.; Ullah, Z.; Sarwono, A.; Shah, F. U.; Muhammad, N. Efficient conversion of lignocellulosic biomass to levulinic acid using acidic ionic liquids. *Carbohydr. Polym.* **2018**, *181*, 208−214.
(32) Wu, Z.; Joo, H.; Lee, K. Kinetics and thermodynamics of the organic dye adsorption on the mesoporous hybrid xerogel. *Chem. Eng. J.* **2005**, *112*, 227−236.
(33) Cooney, D. O. *Adsorption design for wastewater treatment*; CRC Press, 1998.
(34) Naushad, M.; Vasudevan, S.; Sharma, G.; Kumar, A.; Alothman, Z. A. Adsorption kinetics, isotherms, and thermodynamic studies for Hg^{2+} adsorption from aqueous medium using alizarin red-S-loaded amberlite IRA-400 resin. *Desalin. Water Treat.* **2016**, *57*, 18551−18559.
(35) Temkin, M. J.; Pyzhev, V. Recent modifications to Langmuir isotherms. *Acta Physicochim. URSS* **1940**, *12*, 217−225.
(36) Christoforidis, A. K.; Orfanidis, S.; Papageorgiou, S. K.; Lazaridou, A. N.; Favvas, E. P.; Mitropoulos, A. C. Study of Cu(II) removal by Cystoseira crinitophylla biomass in batch and continuous flow biosorption. *Chem. Eng. J.* **2015**, *277*, 334−340.
(37) Shukla, A.; Zhang, Y.-H.; Dubey, P.; Margrave, J. L.; Shukla, S. S. The role of sawdust in the removal of unwantedmaterials from water. *Hazard. Mater.* **2002**, *95*, 137−152.

https://doi.org/10.1021/acsomega.1c02957
ACS Omega 2021, 6, 22259−22271

(38) Ho Lee, S.; Hun Jung, C.; Chung, H.; Yeal Lee, M.; Yang, J.-W. Removal of heavy metals from aqueous solution by apple residues. *Process Biochem.* **1998**, *33*, 205−211.
(39) Krishnani, K.; Meng, X.; Christodoulatos, C.; Boddu, V. Biosorption mechanism of nine different heavy metals onto biomatrix from rice husk. *J. Hazard. Mater.* **2008**, *153*, 1222−1234.
(40) Yao, Z.-Y.; Qi, J.-H.; Wang, L.-H. Equilibrium, kinetic and thermodynamic studies on the biosorption of Cu(II) onto the chestnut shell. *J. Hazard. Mater.* **2010**, *174*, 137−143.
(41) Ajmal, M.; Ali Khan Rao, R.; Anwar, S.; Ahmad, J.; Ahmad, R. Adsorption studies on rice husk: removal and recovery of Cd(II) from wastewater. *Bioresour. Technol.* **2003**, *86*, 147−149.
(42) Al-Othman, Z. A.; Ali, R.; Naushad, M. Hexavalent chromium removal from aqueous medium by activated carbon prepared from peanut shell: adsorption kinetics, equilibrium and thermodynamic studies. *Chem. Eng. J.* **2012**, *184*, 238−247.
(43) Mckay, G. Adsorption of dyestus from aqueous solutions with activated carbon I: equilibrium and batch contact-time studies. *J. Chem. Technol. Biotechnol.* **2007**, *32*, 759−772.
(44) Banat, F.; Al-Asheh, S.; Al-Makhadmeh, L. Utilization of raw and activated date pits for the removal of phenol from aqueous solution. *Chem. Eng. Technol.* **2004**, *27*, 80−86.
(45) Chairat, M.; Rattanaphani, S.; Bremner, J. B.; Rattanaphani, V. An adsorption and kinetic study of lac dyeing on silk. *Dyes Pigm.* **2005**, *64*, 231−241.
(46) Özacar, M.; Şengil, İ. A. A kinetic study of metal complex dye sorption onto pine sawdust. *Process Biochem.* **2005**, *40*, 565−572.
(47) Alkan, M.; Demirbaş, Ö.; Doğan, M. Adsorption kinetics and thermodynamics of an anionic dye onto sepiolite. *Microporous Mesoporous Mater.* **2007**, *101*, 388−396.
(48) Tan, I. A. W.; Ahmad, A. L.; Hameed, B. H. Adsorption isotherms, kinetics, thermodynamics and desorption studies of 2,4,6-trichlorophenol on oil palm empty fruitbunch-based activated carbon. *J. Hazard. Mater.* **2009**, *164*, 473−482.
(49) Dupont, J.; Consorti, C. S.; Suarez, P. A. Z.; Souza, R. F. Preparation of 1-butyl-3-methyl imidazolium based room temperature ionic liquids. *Org. Synth.* **2002**, *79*, 236.

https://doi.org/10.1021/acsomega.1c02957
ACS Omega 2021, 6, 22259−22271